RETROGRADE METAMORPHISM IN THE YAMATO MOUNTAINS, EAST ANTARCTICA

Masao ASAMI[1] and Kazuyuki SHIRAISHI[2]

[1]*Department of Geological Sciences, College of Liberal Arts, Okayama University, 1-1, Tsushima Naka 2-chome, Okayama 700*

[2]*National Institute of Polar Research, 9-10, Kaga 1-chome, Itabashi-ku, Tokyo 173*

Abstract: Retrograde metamorphism which affected the granulite-facies garnet-biotite gneiss and calc-silicate gneiss from Massif A in the Yamato Mountains was petrographically revealed. In the garnet-biotite gneiss, the association of ferruginous matrix biotite (Type I biotite) and magnesian interior of zoned garnet is considered to show the preceded granulite-facies metamorphism because its $K_D^{\text{Bi-Ga}}_{\text{Mg-Fe}}$ value (3.02) suggests an equilibrium temperature of 760°C. On the other hand, the association of magnesian biotite included in garnet (Type II biotite) and the enclosing ferruginous garnet and the association of magnesian biotite (Type III biotite) by which the garnet is partially embayed, fringed or veined and the contacting ferruginous garnet are supposed to show a retrograde metamorphism because their K_D values (about 6.61 and 9.41) suggest the temperatures around 520 and 450°C, respectively. In the calc-silicate gneiss, anorthite (An_{93}) is always enclosed by corona of Ca-garnet or Ca-garnet and quartz, and no anorthite contacts with wollastonite. This suggests stable coexistence of anorthite and wollastonite under the earlier granulite-facies metamorphic conditions, and later development of the corona as retrograde breakdown products.

On the basis of experimental studies of the anorthite-wollastonite equilibria, and two-pyroxene and garnet-biotite thermometries, it is inferred that the granulite-facies metamorphism in the Yamato Mountains took place at about 750°C and below 6 kb. 700 and 500 Ma ages known for the granulite-facies rocks from Massif A might be assigned to the granulite-facies and retrograde metamorphic events, respectively. The granulite-facies metamorphism in the Yamato Mountains can be chronologically correlated with the upper amphibolite- to granulite-facies metamorphism of medium-pressure type in the Prince Olav Coast–Lützow-Holmbukta region, but the former metamorphism should have taken place at a higher crustal level than that in the latter region.

1. Introduction

Retrograde metamorphic effects on pre-existing metamorphic rocks have been reported from many places in the East Antarctic shield and have been assigned to various origins (*e.g.*, TINGEY, 1982; HIROI *et al.*, 1983a, b). Since recrystallization during retrograde metamorphism is more or less incomplete, it is possible to deduce earlier mineral assemblages which reflect conditions of a higher-grade metamorphism; then we can compile the thermal history of each metamorphic terrane.

The Yamato Mountains, situated at about 300 km southwest of Syowa Station

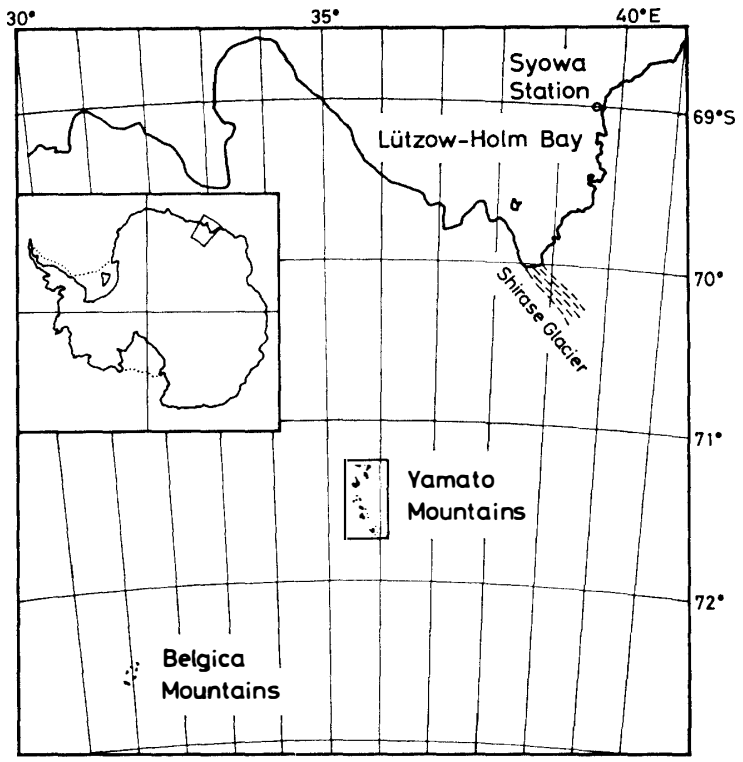

Fig. 1. Location map of the Yamato Mountains.

(Fig. 1), consist mainly of the granulite-facies and amphibolite-facies metamorphic rocks and intrusive syenitic rocks (KIZAKI, 1965; SHIRAISHI, 1977; SHIRAISHI and KIZAKI, 1979; SHIRAISHI *et al.*, 1982, 1983a, b; ASAMI and SHIRAISHI, 1983). KIZAKI (1965) and SHIRAISHI (1977) described hornblende and biotite replacing clinopyroxene in some granulite-facies metamorphic rocks of basic to intermediate composition, and suggested a retrograde metamorphic origin for these two minerals. During our petrological study of this area now in progress, we found a pelitic gneiss and a calcareous gneiss of the granulite-facies in which retrograde mineralogical changes were well-preserved. This paper presents descriptions of these gneisses and brief discussions on retrograde metamorphism and preceded higher-grade metamorphism.

2. Geological Setting

The Yamato Mountains include seven massifs and associated nunataks up to 2494 m in altitude which project above an ice sheet surface of about 2000 m above the sea level and range for 50 km in a N-S direction. The seven massifs have been called provisionally A, B, C, D, E, F and G from south to north (Fig. 2). Since KIZAKI's pioneer work (1965), geology and petrography of the Yamato Mountains have been described in many papers (OHTA and KIZAKI, 1966; YOSHIDA and ANDO, 1971; SHIRAISHI, 1977; SHIRAISHI *et al.*, 1978, 1982, 1983a, b; YANAI *et al.*, 1982; ASAMI and SHIRAISHI, 1983). There mainly occur regional metamorphic rocks and intrusive syenitic rocks, both of which are accompanied by dikes of granitic rocks and

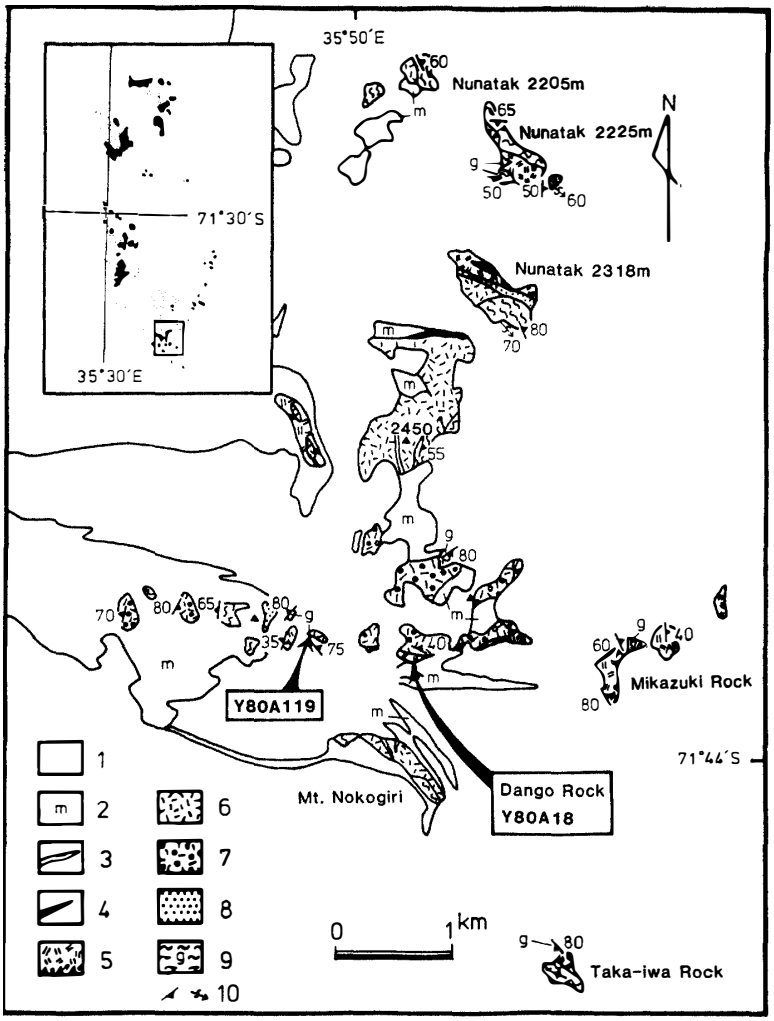

Fig. 2. Geological map of Massif A in the Yamato Mountains. Localities of garnet-biotite gneiss (Y80A119) and calc-silicate gneiss (Y80A18) are also shown. 1. Snow and ice. 2. Morainic debris. 3. Granites and pegmatite. 4. Granitic migmatite. 5. Clinopyroxene quartz monzosyenite; "A" shows agmatitic blocks. 6. Fine-grained massive two-pyroxene syenite. 7. K-feldspar-porphyritic two-pyroxene syenite. 8. Massive quartz syenitic rock. 9. Metamorphic rocks. 10. Foliation and folding axis.

metabasites. According to ASAMI and SHIRAISHI (1983), the metamorphic rocks can be classified into two groups, granulite- and amphibolite-facies rocks, on the basis of the field occurrence and petrographical characters. The granulite-facies rocks occur as two different types: (1) two-pyroxene biotite gneiss and related metamorphics which are intimately associated with the syenitic rocks in Massifs A, D and G, and (2) paleosomes of migmatitic gneiss in Massifs D, E, F and G. On the other hand, the amphibolite-facies rocks consist of granitic gneiss and related metamorphics in Massifs B, C and D. The geological relations between the granulite- and the amphibolite-facies rocks have been inferred to be tectonic, though no clear field evidence has been found (SHIRAISHI *et al.*, 1983a; ASAMI and SHIRAISHI, 1983).

The radiometric ages of the rocks from Massifs A and D have been reported: Rb-Sr whole rock isochron ages of some granulite-facies rocks from Massif A are 718 and 698 Ma (SHIBATA *et al.*, 1985a); a Rb-Sr mineral isochron age of a granulite-facies rock from Massif A is 493 Ma, and K-Ar biotite ages of two granulite-facies rocks from Massif A are 483 and 469 Ma (SHIBATA *et al.*, 1985b); a Rb-Sr biotite age of clinopyroxene syenite from Massif D is 473 Ma (recalculated from 457 Ma after PICCIOTTO and COPPEZ (1964) using a decay constant of $1.42\times10^{-11}y^{-1}$). Thus, two age groups have been known from rocks in the Yamato Mountains.

Figure 2 is a geological map of Massif A. Two kinds of metamorphic rocks, garnet-biotite gneiss (Y80A119) and calc-silicate gneiss (Y80A18), are found in Massif A (Fig. 2) and now studied. The garnet-biotite gneiss occurs as a large xenolithic block enclosed in the fine-grained massive two-pyroxene syenite, and the calc-silicate gneiss as a small sheet-like body in the clinopyroxene quartz monzo-syenite. In the garnet-biotite gneiss, aplitic veins are also present.

3. Petrography and Mineralogy

The mineral compositions were determined using EMPA of JEOL JXA-733. Microprobe analyses were made under such conditions as accelaration voltage of 15 kV, beam currents of about 0.014 μA and a beam diameter of 3 μ. Generally, several grains of each mineral species per specimen and two or more points per grain were analyzed. In the case of the Ca-garnet chemistry, an appropriate amount of iron was calculated as Fe^{3+} to allot for $Al^{VI}+Ti+Cr+Fe^{3+}=4$ on the basis of 24(O), and the remaining iron was treated as Fe^{2+}.

3.1. Garnet-biotite gneiss (Y80A119)

This gneiss is well-banded due to alternation of biotite-rich bands and feldspathic bands. It is composed of quartz, plagioclase, K-feldspar, biotite, garnet, ilmenite and graphite. Garnet occurs as porphyroblasts, up to 5 mm in diameter, in a fine- to medium-grained gneissose matrix. Representative analyses of garnet, biotite, plagioclase and K-feldspar are given in Table 1. Plagioclase and K-feldspar are very rarely zoned and show nearly uniform compositions throughout the specimen, *i.e.* $An_{16.1\text{-}18.0}$ and $Or_{89.2\text{-}91.5}$, respectively.

The modes of occurrence and compositional characters of biotite and garnet in this rock are very interesting. Three types of biotite are distinguishable by the mode of occurrence as shown in Fig. 3. Type I biotite has an axial color of Z=reddish brown. It is common in the matrix and shows preferred orientation parallel to the gneissosity. Type II biotite forms small round grains which are included in garnet and have the same *Z*-axial color as Type I. Type II biotite is found not only in the central part but also near the rim of garnet grains. Type III biotite occurs in such a mode that garnet is partially embayed, fringed or veined. Its axial color is Z=pale yellowish brown to very pale yellowish green. Corresponding to the modes of occurrence, these biotites are different in chemical composition from one type to the other, particularly in Fe/Fe+Mg ratio (X_{Fe}) and TiO_2 content as shown in Table 1 and Fig. 4. Figure 4 indicates that Type I is high in both X_{Fe} and TiO_2 content, Type II

Table 1. Representative analyses of minerals in garnet-biotite gneiss.

	Garnet			Biotite				K-feldspar		Plagioclase	
	Core	Rim D	Rim A	Type I	Type II	Type III-a	Type III-b	Core	Rim	Core	Rim
SiO_2	37.53	36.71	37.23	35.07	36.13	36.73	36.76	63.53	63.80	63.10	63.09
TiO_2	0.03	0.03	0.01	3.96	5.44	1.52	0.21	0.01	0.00	0.07	0.01
Al_2O_3	21.15	20.90	21.33	16.84	16.30	17.40	18.10	18.41	18.26	22.52	22.38
Cr_2O_3	0.00	0.00	0.00	0.01	0.00	0.03	0.03	0.00	0.03	0.00	0.00
FeO*	31.98	34.27	34.89	18.71	13.83	13.07	13.38	0.00	0.05	0.00	0.00
MnO	1.64	1.76	2.27	0.00	0.03	0.05	0.03	0.05	0.00	0.00	0.00
MgO	5.96	5.30	3.75	10.53	13.34	15.41	15.28	0.00	0.00	0.00	0.00
CaO	0.75	0.64	0.75	0.01	0.00	0.01	0.02	0.01	0.00	3.82	3.82
Na_2O	0.02	0.03	0.00	0.08	0.58	0.19	0.07	1.05	0.91	9.64	9.64
K_2O	0.00	0.01	0.02	9.26	9.14	9.33	9.28	14.54	14.85	0.33	0.11
Total	99.06	99.65	100.25	94.47	94.79	93.74	93.16	97.60	97.90	99.48	99.05
		24(O)				22(O)		32(O)		32(O)	
Si	5.992	5.906	5.970	5.387	5.402	5.511	5.544	11.961	11.988	11.232	11.262
Al	3.974	3.963	4.030	3.049	2.872	3.077	3.218	4.086	4.044	4.725	4.708
Ti	0.004	0.003	0.002	0.458	0.612	0.171	0.024	0.001	—	0.010	0.001
Cr	—	—	—	0.001	—	0.003	0.003	—	0.004	—	—
Fe	4.269	4.611	4.678	2.404	1.729	1.640	1.688	—	0.007	—	—
Mn	0.222	0.240	0.308	—	0.004	0.007	0.004	0.008	—	—	—
Mg	1.419	1.270	0.896	2.411	2.974	3.448	3.437	—	—	—	—
Ca	0.127	0.110	0.129	0.001	0.001	0.001	0.003	0.002	—	0.729	0.730
Na	0.005	0.008	—	0.024	0.168	0.054	0.020	0.384	0.331	3.327	3.337
K	—	0.003	0.004	1.814	1.743	1.787	1.786	3.491	3.559	0.074	0.025
Fe/Fe +Mg	0.751	0.784	0.839	0.499	0.368	0.322	0.329				
Al	70.7	74.0	77.8								
Py	23.5	20.4	14.9								
Sp	3.7	3.9	5.1								
Gr	2.1	1.8	2.1								
An								0.1	0.0	17.7	17.8
Ab								9.9	8.5	80.6	81.6
Or								90.0	91.5	1.8	0.6

* Total iron as FeO. Types I and II: Z=reddish brown. Type III-a and b: Z=pale yellowish brown and very pale yellowish green, respectively.

is low in X_{Fe} but high in TiO_2 as Type I, and Type III is low in both the values. In this case, the reddish Z-axial color of biotite may be mainly attributed to the high TiO_2 content as exemplified in Table 1.

Garnet depicted in Fig. 3 appears to be a single porphyroblast, though it is now separated into two grains. This is also suggested by the pattern of compositional zoning shown in Fig. 5a. Chemical compositions of the garnet porphyroblast were examined along two lines crossing at high angles, A–D and E–J (Fig. 3). The edges A, E, F, G, H, I and J are in contact with biotite of Type III and B, C and D in contact with quartz. Compositional profiles along the two lines are shown in Figs. 5a and 5b. Line E–J traverses two biotite grains of Type III at F–G and H–I.

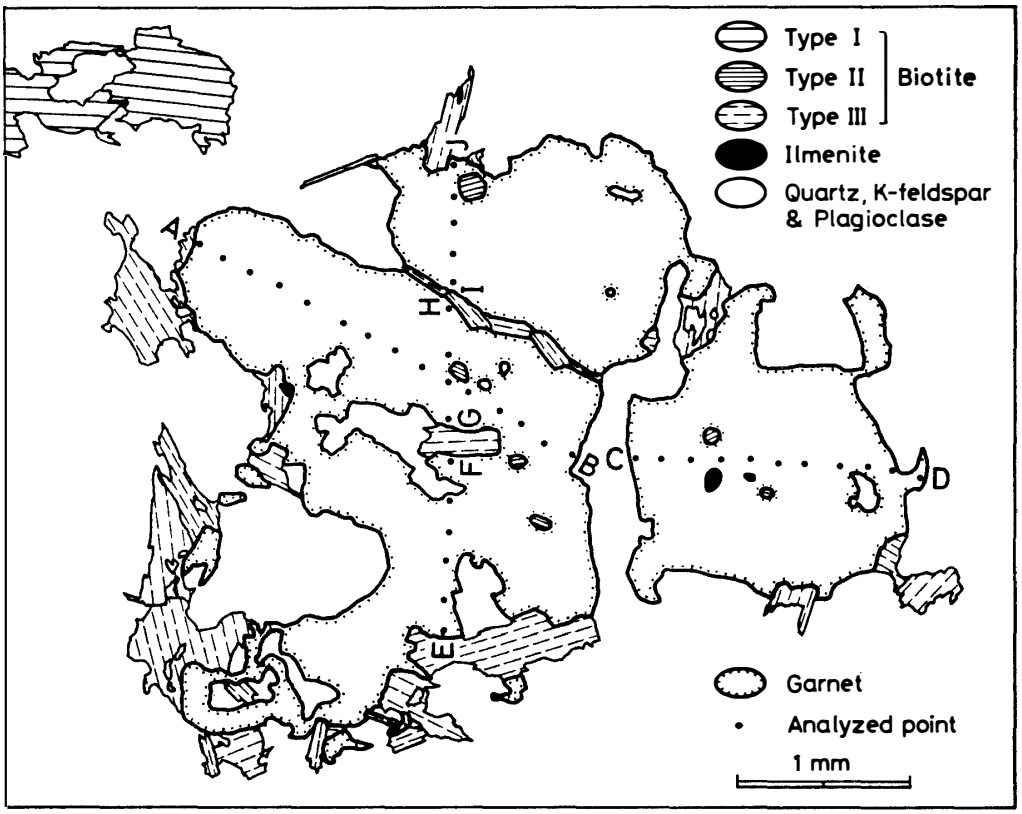

Fig. 3. Sketch showing modes of occurrence of a garnet porpyroblast and three types of biotite in the garnet-biotite gneiss.

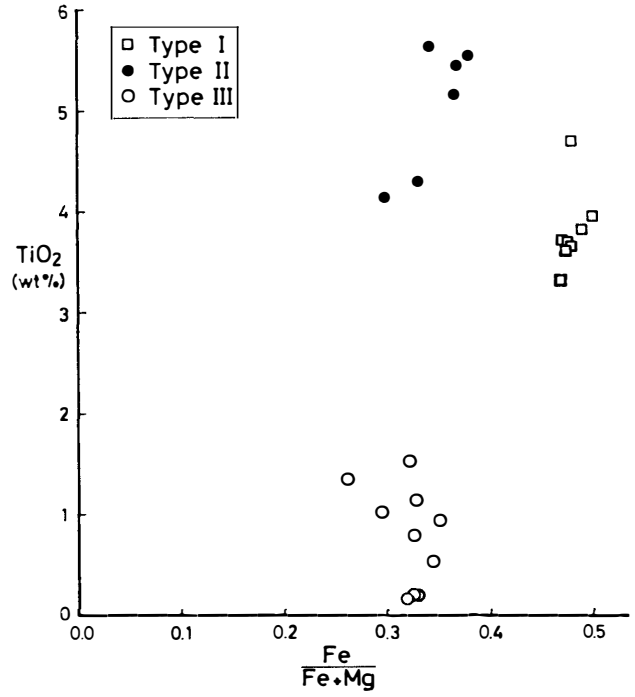

Fig. 4. X_{Fe}-TiO_2 diagram for three types of biotite.

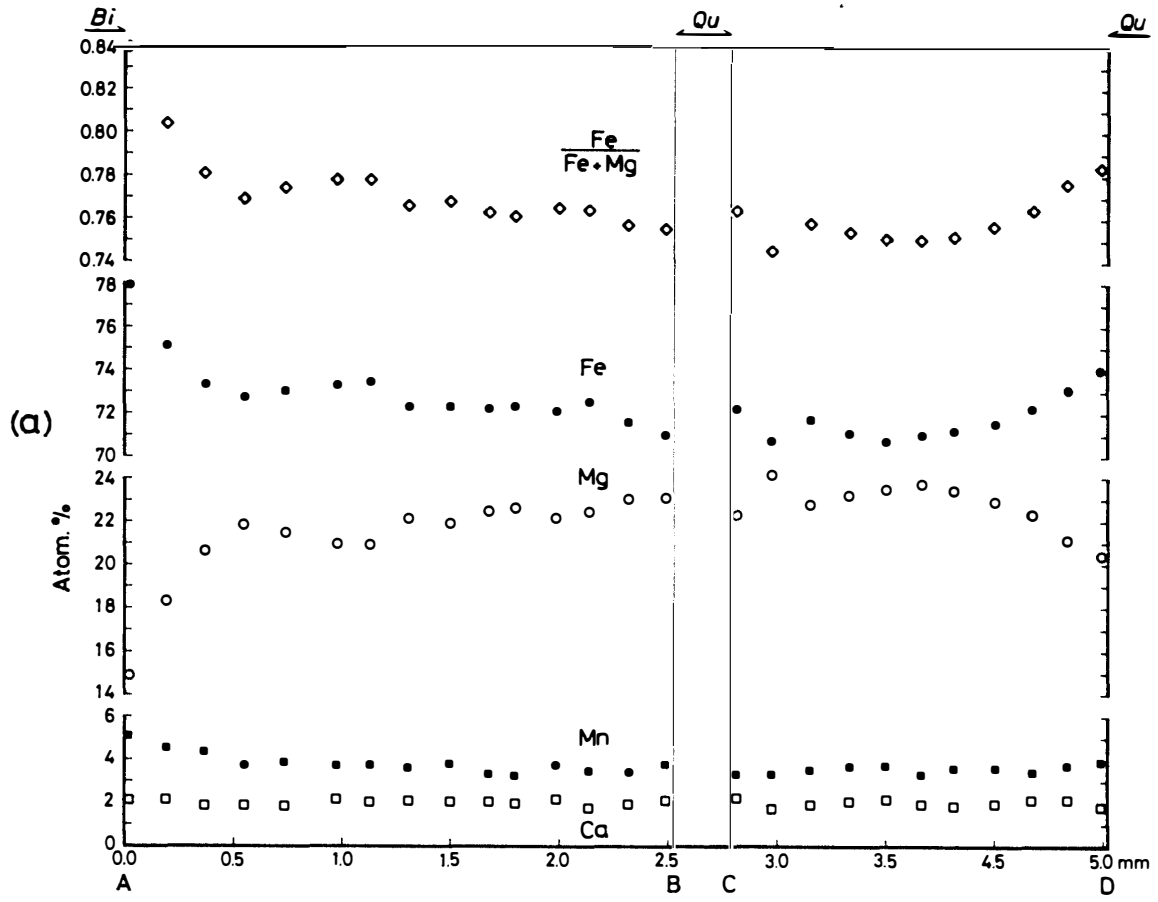

(*a*) *Along line A–D.*

Fig. 5. Compositional profiles of the garnet shown in Fig. 3.

In both profiles, the Mn and Ca contents of garnet are very low and almost uniform from one side to the other except a slight increase of Mn near the contact with Type III biotite. The Fe content of garnet increases abruptly with approach to rim A and D (Fig. 5a), particularly at A where the garnet is in contact with Type III biotite. Figure 5b also exhibits a similar tendency of Fe-enrichment near the contact with Type III biotite, regardless of rim or interior of garnet (E, F, G, H, I and J). In both profiles, the Mg content varies but balances the Fe content due to the uniformities of the Mn and Ca contents. As a result, Fe/Fe+Mg ratios (X_{Fe}) of the garnet become higher near the rim and near other edges contacting with Type III biotite, while they are nearly uniform at the interior of garnet (0.75–0.77). Near the contact of garnet with Type II biotite, no marked compositional variation of the garnet can be observed (Figs. 3 and 5).

3.2. Calc-silicate gneiss (Y80A18)

This is a light gray, fine to medium-grained and faintly gneissose rock. Wollastonite, plagioclase, scapolite and clinopyroxene are found as major constituents of the gneiss, and garnet, quartz, sphene and apatite as minor ones. Clinopyroxene is pale green and weakly pleochroic. Representative analyses of plagioclase, scapolite, wollastonite, clinopyroxene and garnet are listed in Table 2. Plagioclase is nearly

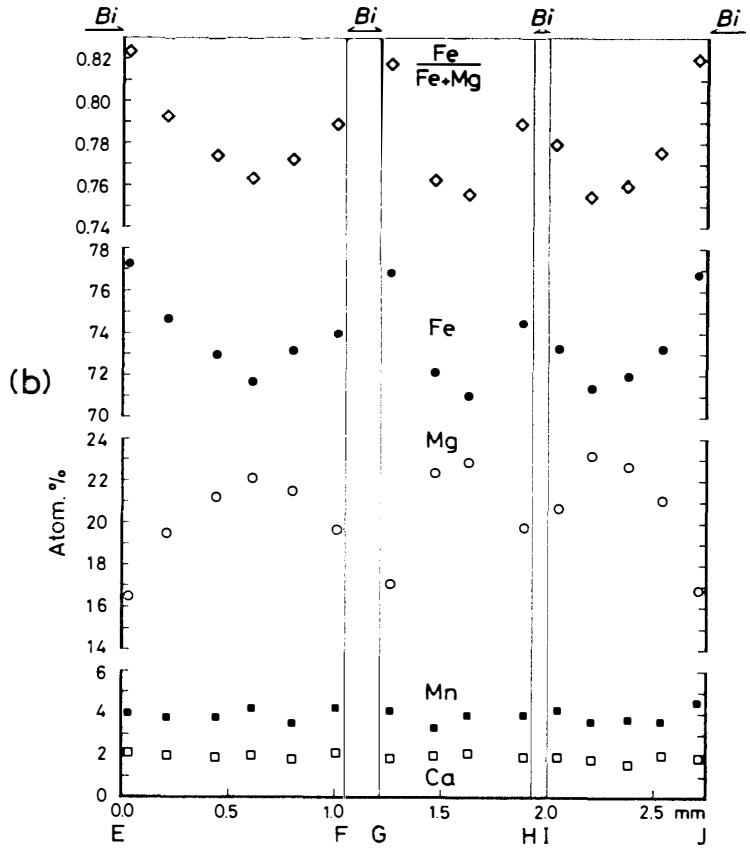

(*b*) *Along line E–J.*

Fig. 5. Compositional profiles of the garnet shown in Fig. 3.

homogeneous in composition within each grain and between grains, and is anorthite ($An_{91.5-93.5}$). Scapolite shows some compositional variations among grains, from $Me_{60.7}$ to $Me_{74.2}$. Wollastonite contains FeO of 0.37–0.75 wt% and MnO of 0.14–0.37 wt%. Clinopyroxene is ferrosalite with $X_{Fe}=0.74$–0.78, Al_2O_3 of 0.66–1.22 wt% and MnO of 0.40–0.64 wt%. Garnet is grossularous one with considerable amounts of the andradite component ($Gr_{71.2-74.0}Ad_{20.6-17.6}Uv_{0.0}Al_{6.9-6.8}Py_{0.3}Sp_{1.1-1.4}$).

Most noticeable in the calc-silicate gneiss is textural relations involving anorthite, scapolite, wollastonite, ferrosalite, garnet and quartz. Examples showing their modes of occurrence are displayed in Fig. 6. Anorthite, scapolite, wollastonite and ferrosalite are mostly granoblastic in appearance, whereas garnet is developed always along anorthite-wollastonite boundaries and often along scapolite-wollastonite, anorthite-ferrosalite and scapolite-ferrosalite boundaries. Quartz is found, though not always present, along boundaries of wollastonite-garnet, wollastonite-wollastonite, wollastonite-ferrosalite and scapolite-wollastonite. That is to say, no anorthite is just in contact with wollastonite and also with quartz. On the other hand, anorthite is in contact with scapolite, and wollastonite is in contact with ferrosalite. Scapolite is rarely in contact with ferrosalite and wollastonite, and anorthite is also rarely in contact with ferrosalite. Small grains of sphene and apatite are in contact with all of the other constituents.

Table 2. Representative analyses of minerals in calc-silicate gneiss.

	Plagioclase		Scapolite	Wollastonite	Clinopyroxene	Garnet
	Core	Rim				
SiO_2	44.39	44.15	46.15	51.19	49.85	38.26
TiO_2	0.00	0.02	0.00	0.03	0.03	0.24
Al_2O_3	34.92	35.12	27.76	0.00	0.66	18.30
Cr_2O_3	0.03	0.01	0.00	0.00	0.01	0.00
Fe_2O_3**						9.25
FeO*	0.07	0.17	0.07	0.53	21.15	
MnO	0.00	0.00	0.00	0.29	0.59	0.64
MgO	0.00	0.00	0.00	0.00	4.28	0.07
CaO	18.73	19.12	17.92	48.09	23.34	33.06
Na_2O	0.85	0.88	3.35	0.01	0.11	0.00
K_2O	0.04	0.00	0.42	0.00	0.00	0.02
Total	99.03	99.47	95.67	100.14	100.02	99.84
	32(O)		12(Si+Al)	6(O)	6(O)	24(O)
Si	8.282	8.218	7.022	1.986	1.986	5.945
Al	7.679	7.705	4.978	—	0.031	3.351
Ti	—	0.002	—	0.001	0.001	0.028
Cr	0.005	0.001	—	—	—	—
Fe^{3+}						0.676
Fe^{2+}	0.010	0.026	0.008	0.017	0.705	0.406
Mn	—	—	—	0.009	0.020	0.084
Mg	—	—	—	—	0.254	0.016
Ca	3.744	3.814	2.922	1.999	0.996	5.504
Na	0.306	0.318	0.989	0.001	0.008	0.006
K	0.009	0.001	0.081	—	—	—
	$An_{92.2}$	$An_{92.3}$	$Me_{73.3}$	$Wo_{99.2}$	$Wo_{50.9}$	$Gr_{74.0}$
	$Ab_{7.6}$	$Ab_{7.7}$		$En_{0.0}$	$En_{13.0}$	$Ad_{17.6}$
	$Or_{0.2}$	$Or_{0.0}$		$Fs_{0.8}$	$Fs_{36.1}$	$Uv_{0.0}$
						$Al_{6.8}$
						$Py_{0.3}$
						$Sp_{1.4}$

* Total iron as FeO. ** Total iron as Fe_2O_3.

4. Retrograde Metamorphic Effects and Conditions

The mode of occurrence of Type III biotite suggests that the garnet porphyroblast was replaced partially by biotite at the rim. If atomic diffusion within the garnet was insufficient at a later metamorphic stage, Mn should be relatively enriched near the replaced edges of the garnet because Mn is much more concentrated in garnet than biotite (ALBEE, 1972; THOMPSON, 1976a). In the present case, however, Mn-enrichment near the contact with Type III biotite is generally inconspicuous (Fig. 5). Thus, the replacement of the garnet by the biotite was probably small in extent.

X_{Fe} of garnet in this rock may be fixed by Fe-Mg exchange reaction with biotite, because biotite is a sole main Fe-Mg constituent except garnet. Thus, the increase of X_{Fe} at the garnet rim and at other edges contacting with Type III biotite and lower

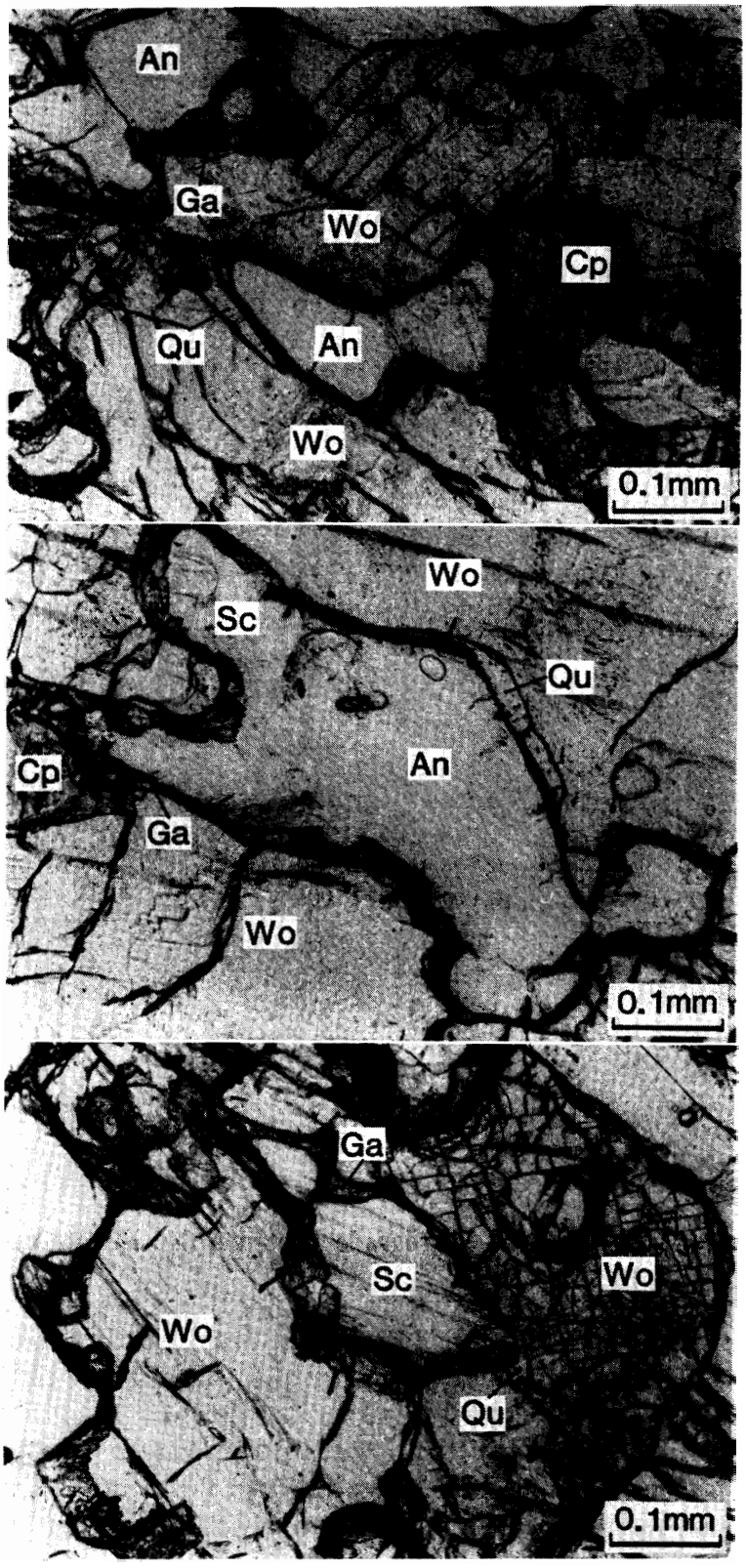

a. Anorthite (An) is completely enclosed by Ca-garnet (Ga) and quartz (Qu) which are developed along the boundary between anorthite and both wollastonite (Wo) and ferrosalite (Cp). Wollastonite and ferrosalite are directly in contact with each other. One nicol.

b. Anorthite and scapolite (Sc) are in mutual contact, but both are entirely enclosed by Ca-garnet and quartz. Surroundings are wollastonite and ferrosalite. One nicol.

c. Scapolite enclosed by Ca-garnet in the same manner as anorthite. One nicol.

Fig. 6. Photomicrographs showing modes of occurrence of some constituents in the calc-silicate gneiss.

X_{Fe} of Type III biotite suggest that the new Fe-Mg distribution was fixed under lower temperature conditions than those of the rest, refractory interior, of the garnet. The refractory interior of the garnet may represent the compositions of granet which would have coexisted with Fe-rich Type I biotite under the granulite-facies conditions. It is considered that the increase of X_{Fe} in the garnet noted above and the development of Type III biotite reflect retrograde metamorphic effects.

Unlike Type III biotite, the mode of occurrence and high TiO_2 content of Type II biotite suggest that Type II biotite grew with the garnet porphyroblast during an earlier higher-grade metamorphic stage. However, Type II biotite is more magnesian than the matrix biotite (Type I). HESS (1971) and KANISAWA and YANAI (1982) reported such examples that biotite included in homogeneous garnet is more magnesian than that in the matrix. They interpreted that the included biotite was seized by the growing garnet at an earlier stage of metamorphism and the compositions of the biotite were kept unchanged through later prograde metamorphism. In the garnet-biotite gneiss, the Mg/Fe values of Type II biotite appear to depend only on those of enclosing garnet, even near the garnet rim where the outward increase of X_{Fe} suggesting a retrograde effect (near J in Fig. 3) is observed; that is, the K_{DMg-Fe} values between them are kept constant as indicated by Fig. 7. More magnesian compositions of Type II biotite than Type I biotite now observed may be attributed to retrograde Fe-Mg exchange between the biotite and the enclosing garnet.

The X_{Fe} values and the TiO_2 contents of biotites in the garnet-biotite gneiss vary even in each type as shown in Fig. 4, so that biotites of each type seem to be

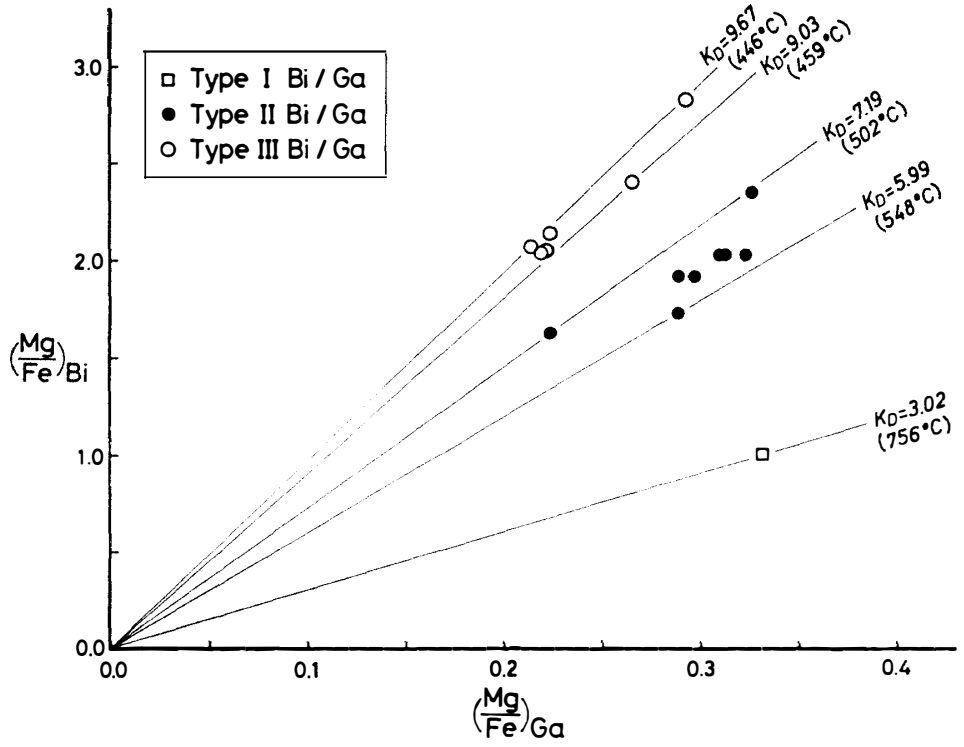

Fig. 7. Mg-Fe distributions between biotite and garnet. Equilibrium temperatures are based upon THOMPSON's garnet-biotite thermometer (1976).

mutually in disequilibrium as a whole. However, if Fe-Mg exchange equilibrium between biotite and enclosing garnet was locally attained at any temperature and Fe-Mg mixing was ideal, the distribution coefficient $K_D^{\text{Bi-Ga}}_{\text{Mg-Fe}}$ should be constant despite their variable X_{Fe} values. Figure 7 shows the Mg/Fe distributions between biotite of Types II and III and the contacting garnet. Six Mg/Fe plots for Type III biotite and contacting garnet give a narrow range of K_D values such as 9.03–9.67 (9.41 on the average). Similarly, eight plots for Type II biotite and the contacting garnet show limited K_D from 5.99 to 7.19 (6.61 on the average), though those values are lower than those of Type III biotite. These facts suggest an approach to local equilibrium between biotites of the two types and the contacting garnets. According to THOMPSON's garnet-biotite geothermometer (1976b), equilibrium temperatures of 440–460°C (*ca.* 450°C in average) are obtained for the Type III biotite-garnet pairs and those of 500–550°C (*ca.* 520°C on the average) for the Type II biotite-garnet pairs.

As stated above, Type III biotite is different in TiO_2 content from Type II biotite and also from Type I biotite (Fig. 4). Several types of Ti substitution are known for natural biotite (INDARES and MARTIGNOLE, 1985). Tetrahedral Si contents in biotites of the three types are approximately invariable as exemplified in Table 1 and show no correlation with varying octahedral Ti contents, so that Ti substitution in the biotites would not be due to such ways as $(R^{2+})^{VI}+2Si^{IV}=Ti^{VI}+2Al^{IV}$ and $Al^{VI}+Si^{IV}=Ti^{VI}+Al^{IV}$. The Ti contents are plotted against total octahedral cations in Fig. 8. Total octahedral cations tend to decrease with increasing Ti content. Such a tendency suggests that Ti substitution is mainly due to the substitutional reaction $2(R^{2+})^{VI}=Ti^{VI}+(\ )^{VI}$. Ti substitution of this type may yield a volume decrease, which is compensated by the replacement of Mg ions by larger Fe^{2+} ions, and the corre-

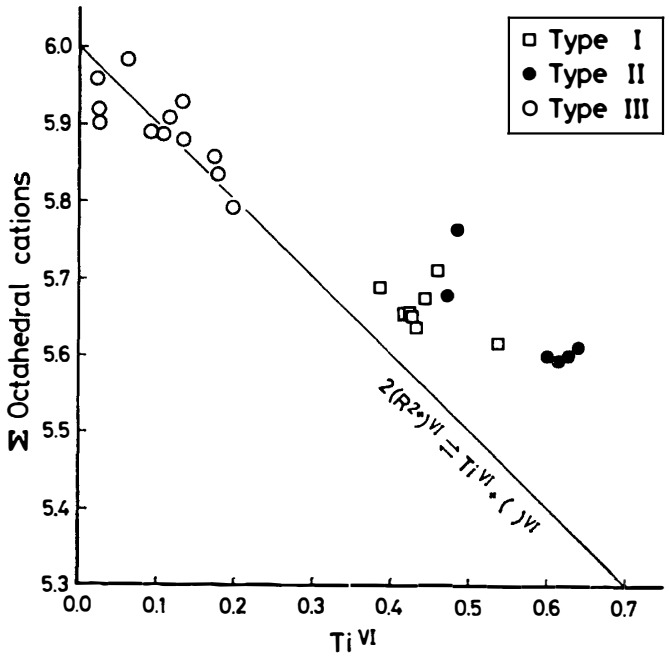

Fig. 8. Octahedral Ti-total octahedral cations diagram for biotite in the garnet-biotite gneiss.

sponding increase in Fe/Mg ratio results in an increase in T_{Ga-Bi} calculated using an ideal model (INDARES and MARTIGNOLE, 1985). THOMPSON's thermometer is based on data of natural garnets and biotites, and the latters contain moderate amounts of TiO_2 (*e.g.*, GUIDOTTI, 1974). Compared with these biotites, Type II biotite is considerably high in TiO_2 content and Type III biotite is somewhat low. Thus, 520°C for Type II-garnet pair and 450°C for Type III biotite-garnet pair may represent values rather higher and lower, respectively, than actual equilibrium temperatures. It is inferred from the above discussion that the retrograde mineralogical changes in the garnet-biotite gneiss took place between 520 and 450°C.

The modes of occurrence and contact relationships of the minerals in the calc-silicate gneiss as described in the previous section suggest that garnet and quartz are reaction products and the other minerals except garnet and quartz are those which have stably coexisted at the earlier metamorphic stage. Judging from the textural relations, scapolite and ferrosalite should have participated in the garnet-quartz-forming reaction. However, the most essential reaction may be explained by the

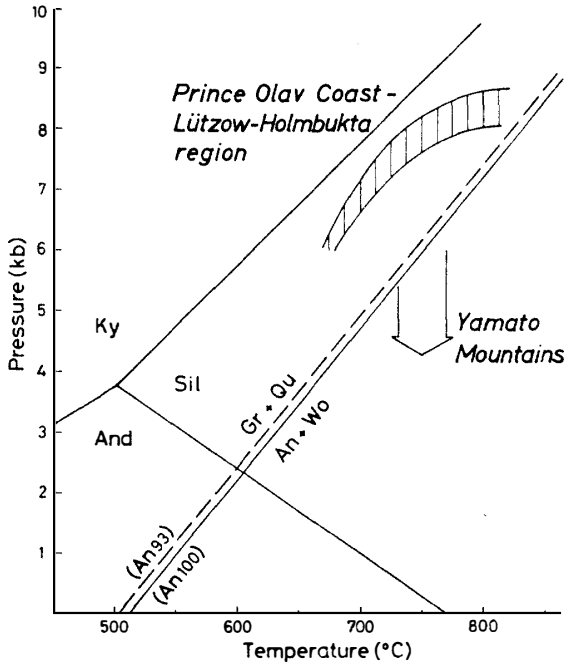

Fig. 9. P-T diagram for the reaction grossular + quartz = anorthite + wollastonite. The reaction curve (An_{100}) represents experimental results obtained for the minerals of pure composition (WINDOM and BOETTCHER, 1976). The curve (An_{93}) is a calculated result obtained on the basis of the curve (An_{100}) when $X_{An}^{Pl} = 0.93$. The granulite-facies metamorphic conditions in the Yamato Mountains are estimated to be around 750°C and below 6 kb, whose lower-pressure character is compared with the higher-pressure one of upper amphibolite- to granulite-facies metamorphism in the Prince Olav Coast–Lützow-Holmbukta region (HIROI et al., 1984). The stability of aluminosilicates (HOLDAWAY, 1971) is shown for comparison.

reaction (1), because anorthite and wollastonite are always isolated by corona composed of garnet and quartz.

$$\text{anorthite} + \text{wollastonite} \longrightarrow \text{grossular} + \text{quartz} \qquad (1)$$

This means that *T-P* conditions at the later metamorphic stage were at least beyond the stability field of anorthite (An_{93}) plus wollastonite.

NEWTON (1966), BOETTCHER (1970) and WINDOM and BOETTCHER (1976) experimentally determined the equilibrium relation of the reaction (2).

$$\underset{\text{grossular}}{Ca_3Al_2Si_3O_{12}} + \underset{\text{quartz}}{SiO_2} = \underset{\text{anorthite}}{CaAl_2Si_2O_8} + \underset{\text{wollastonite}}{2CaSiO_3} \qquad (2)$$

The experimental results are shown in Fig. 9. In the calc-silicate gneiss now concerned, wollastonite is very close to pure composition, while anorthite is An_{93}. WINDOM and BOETTCHER (1976) obtained $\gamma_{An}^{Pl}=1.0$ for the composition range of An_{80-100} at 1100°C. Assuming $\gamma_{An}^{Pl}=1.0$, the equilibrium pressure of the reaction (2) increases with decrease in An content; for example, with changing compositions from An_{100} to An_{93} the pressure difference is calculated to be about 0.2 kb at 750°C (Fig. 8). This means that the stability limit of anorthite (An_{93})-wollastonite pair coincides actually with that of pure anorthite-wollastonite pair. The reaction (1) is possible to take place not only with decreasing temperature but also with increasing pressure. In the present case, breakdown of the assemblage anorthite-wollastonite is ascribable to decreasing temperature because retrograde metamorphism suggested by the petrographical characters of the garnet-biotite gneiss must have controled the calc-silicate gneiss and the temperatures of 450–520°C are low enough to stabilize the assemblage grossular-quartz.

5. Preceded Granulite-facies Metamorphism

Retrograde metamorphism recognized in the garnet-biotite gneiss and the calc-silicate gneiss left many refractory minerals unchanged. By eliminating the later effects from the rocks, it is possible to infer mineral parageneses produced during a preceded metamorphism.

$K_{DMg\text{-}Fe}$ between the matrix biotite (Type I) and the Mg-richest interior of the garnet in the garnet-biotite gneiss may be considered to be close to the value of the granulite-facies metamorphism. The Mg/Fe ratios of the two minerals are also plotted in Fig. 7 and give $K_D=3.02$, which is lower than the values calculated for biotite of Types II and III. An equilibrium temperature of 760°C is estimated from the value using THOMPSON's calibration curve (1976b). This is consistent with the temperatures of 730–770°C obtained for two-pyroxene pairs in the basic to intermediate metamorphic rocks from the Yamato Mountains (ASAMI and SHIRAISHI, 1983). The original constituent minerals which coexisted at the granulite-facies metamorphic stage were garnet of $X_{Fe}=0.75$, Type I biotite, K-feldspar, plagioclase, quartz, ilmenite and graphite.

In the calc-silicate gneiss, anorthite (An_{93}) and wollastonite, which are now isolated by corona of garnet and quartz, must have coexisted stably with each other and also

with scapolite and clinopyroxene during the preceded granulite-facies metamorphism. On the basis of the experimental results of the reaction (2) shown in Fig. 9, the anorthite-wollastonite pair defines a maximum solid pressure during metamorphism if a metamorphic temperature is known. Taking 750°C as temperature of the granulite-facies metamorphism of this area, pressures less than 6 kb obtained.

It has been known that the granulite-facies metamorphism in the Lützow-Holmbukta region, situated 200–300 km northeast of the Yamato Mountains, is of medium-pressure type (HIROI *et al.*, 1983a, b) and its pressure conditions are 6–10 kb (SUZUKI, 1983; YOSHIDA and AIKAWA, 1983; MOTOYOSHI *et al.*, 1985). The calcareous metamorphic rocks in the Lützow-Holmbukta region contain the association of Ca-rich garnet and quartz instead of anorthite and wollastonite (SUZUKI and MORIWAKI, 1979; SUZUKI, 1984), suggesting higher metamorphic pressures than those in the Yamato Mountains (Fig. 9).

SHIBATA *et al.* (1985a) presented Rb-Sr whole rock isochron ages of 718 and 696 Ma for some specimens of the granulite-facies gneiss from Massif A of the Yamato Mountains, and SHIBATA *et al.* (1985b) gave a Rb-Sr mineral isochron age of 493 Ma and a K-Ar biotite age of 469 Ma to one of these specimens. The mineral isochron age indicates that constituent minerals of the gneiss were almost completely homogenized in respect to Sr isotopes at about 500 Ma, and the age suggests the last stage of metamorphism of the Yamato Mountains (SHIBATA *et al.*, 1985b). Retrograde metamorphism in Massif A is likely to have taken place under the temperature conditions of 450–520°C, which are considered high enough for the Sr-isotopic homogenization among constituent minerals. Thus, the 500 Ma age might correspond to the retrograde metamorphic event in the granulite-facies terrain of this area. In the same manner, the whole rock isochron age of 700 Ma possibly indicates the age of the granulite-facies metamorphism. However, whether these two events are of polymetamorphic origin or represent plural phases of one metamorphism is not known at present.

Similar chronological results, about 700 Ma and 400–500 Ma, have been known in the Prince Olav Coast–Lützow-Holmbukta region (SHIBATA *et al.*, 1985a, b). HIROI *et al.* (1983a, b) assinged the 400–500 Ma metamorphic event mainly to thermal metamorphism accompanying the granite-pegmatite intrusions of 400–500 Ma. If the 700 Ma event is correlated with the upper amphibolite- to granulite-facies regional metamorphism in the Prince Olav Coast–Lützow-Holmbukta region, it is plausible to regard the Yamato Mountains as an extension of the metamorphic terrains developed at about 700 Ma. In this case, however, 700 Ma rocks in the Yamato Mountains appear to have been formed at a higher crustal level than rocks in the Lützow-Holmbukta region, as suggested by the difference in metamorphic pressure between the two areas (Fig. 8).

Acknowledgments

We wish to thank Prof. T. NUREKI of Okayama University for his critical reading of the manuscript. Thanks are also due to Dr. Y. OHTA of Norsk Polarinstitutt for his co-operation in the field and Mr. H. KOJIMA of National Institute of Polar

Research and Mr. Y. MOTOYOSHI of Hokkaido University for their help during microprobe analyses.

References

ALBEE, A. L. (1972): Metamorphism of pelitic schists; Reaction relations of chloritoid and staurolite. Geol. Soc. Am. Bull., **83**, 3249–3268.

ASAMI, M. and SHIRAISHI, K. (1983): Mineral parageneses of basic to intermediate metamorphic rocks in the Yamato Mountains, East Antarctica. Mem. Natl Inst. Polar Res., Spec. Issue, **28**, 198–214.

BOETTCHER, A. L. (1970): The system CaO-Al_2O_3-SiO_2-H_2O at high pressures and temperatures. J. Petrol., **11**, 337–379.

GUIDOTTI, C. V. (1974): Transition from staurolite to sillimanite zone, Rangeley quadrangle, Maine. Geol. Soc. Am. Bull., **85**, 475–490.

HESS, P. C. (1971): Prograde and retrograde equilibria in garnet-cordierite gneiss in south-central Massachusetts. Contrib. Mineral. Petrol., **30**, 177–195.

HIROI, Y., SHIRAISHI, K., YANAI, K. and KIZAKI, K. (1983a): Aluminum silicates in the Prince Olav and Sôya Coasts, East Antarctica. Mem. Natl Inst. Polar Res., Spec. Issue, **28**, 115–131.

HIROI, Y., SHIRAISHI, K., NAKAI, Y., KANO, T. and YOSHIKURA, S. (1983b): Geology and petrology of Prince Olav Coast, East Antarctica. Antarctic Earth Science, ed by R. L. OLIVER *et al.* Canberra, Aust. Acad. Sci., 32–35.

HIROI, Y., SHIRAISHI, K., MOTOYOSHI, Y. and YANAI, K. (1984): Syowa Kiti shûhen ni bunpu suru genseidai henseigan-rui no keisei ni taisuru purêto tekutonikku moderu (Plate tectonic model for development of Proterozoic metamorphic rocks around Syowa Station). Dai-5-kai Nankyoku Chigaku Sinpojiumu Puroguramu・Kôen Yôshi (Program・Abstr. 5th Symp. Antarct. Geosci.), Tokyo, Natl Inst. Polar Res., 42–43.

HOLDAWAY, M. J. (1971): Stability of andalusite and the aluminum silicate phase diagram. Am. J. Sci., **271**, 97–131.

INDARES, A. and MARTIGNOLE, J. (1985): Biotite-garnet geothermometry in the granulite facies; The influence of Ti and Al in biotite. Am. J. Sci., **70**, 272–278.

KANISAWA, S. and YANAI, K. (1982): Metamorphic rocks of the Cape Hinode district, East Antarctica. Mem. Natl Inst. Polar Res., Spec. Issue, **21**, 71–85.

KIZAKI, K. (1965): Geology and petrography of the Yamato Sanmyaku, East Antarctica. JARE Sci. Rep., Ser. C (Geol.), **3**, 27 p.

MOTOYOSHI, Y., MATSUBARA, S., MATSUEDA, H. and MATSUMOTO, Y. (1985): Garnet-sillimanite gneisses from the Lützow-Holm bay region, East Antarctica. Mem. Natl Inst. Polar Res., Spec. Issue, **37**, 82–94.

NEWTON, R. C. (1966): Some calc-silicate equilibrium relations. Am. J. Sci., **264**, 204–222.

OHTA, Y. and KIZAKI, K. (1966): Petrographic studies of potash feldspar from the Yamato Sanmyaku, East Antarctica. JARE Sci. Rep., Ser. C (Geol.), **5**, 40 p.

PICCIOTO, E. and COPPEZ, A. (1964): Bibliographie des mesures d'ages absolus en Antarctique. Ann. Soc. Geol. Belg., **87**, 115–128.

SHIBATA, K., YANAI, K. and SHIRAISHI, K. (1985a): Syowa Kiti shûhen-san henseigan no Rb-Sr zengan nendai (Rb-Sr whole-rock isochron ages of the metamorphic rocks from around Syowa Station). Ganseki Kôbutsu Kôshô Gakkaishi (J. Jpn. Assoc. Mineral. Petrol. Econ. Geol.), **80**, 172.

SHIBATA, K., YANAI, K. and SHIRAISHI, K. (1985b): Rb-Sr mineral isochron ages of metamorphic rocks around Syowa Station and from the Yamato Mountains, East Antarctica. Mem. Natl Inst. Polar Res., Spec. Issue, **37**, 164–171.

SHIRAISHI, K. (1977): Geology and petrography of the northern Yamato Mountains, East Antarctica. Mem. Natl Inst. Polar Res., Ser. C (Earth Sci.), **12**, 33 p.

SHIRAISHI, K and KIZAKI, K. (1979): Yamato Sanmyaku no chishitsu (Geology of the Yamato Mountains). Gekkan Chikyu (The Earth Monthly), **1**, 928–937.

SHIRAISHI, K., KIZAKI, K., YOSHIDA, M. and MATSUMOTO, Y. (1978): Mt. Fukushima, northern Yamato Mountains. Antarct. Geol. Map Ser., Sheet 27 (1) (with explanatory text 7 p, 2 pl.). Tokyo, Natl Inst. Polar Res.

SHIRAISHI, K., ASAMI, M. and OHTA, Y. (1982): Plutonic and metamorphic rocks of Massif-A in the Yamato Mountains, East Antarctica. Mem. Natl Inst. Polar Res., Spec. Issue, **21**, 21–31.

SHIRAISHI, K., ASAMI, M. and OHTA, Y. (1983a): Geology and petrology of the Yamato Mountains. Antarctic Earth Science, ed. by R. L. OLIVER *et al.*, Canberra, Aust. Acad. Sci., 50–53.

SHIRAISHI, K., ASAMI, M. and KANAYA, H. (1983b): Petrochemical character of the syenitic rocks from the Yamato Mountains, East Antarctica. Mem. Natl Inst. Polar Res., Spec. Issue, **28**, 183–197.

SUZUKI, M. (1983): Preliminary note on the metamorphic conditions around Lützow-Holm Bay, East Antarctica. Mem. Natl Inst. Polar Res., Spec. Issue, **28**, 132–143.

SUZUKI, M. (1984): Reexamination of metapelites in the Cape Omega area, westernmost part of Prince Olav Coast, East Antarctica. Mem. Natl Inst. Polar Res., Spec. Issue, **33**, 145–154.

SUZUKI, M. and MORIWAKI, K. (1979): Cape Omega. Antarct. Geol. Map Ser., Sheet 21 (with explanatory text 5 p., 2 pl.). Tokyo, Natl Inst. Polar Res.

THOMPSON, A. B. (1976a): Mineral reactions in pelitic rocks; I. Prediction of P-T-X (Fe-Mg) phase relations. Am. J. Sci., **276**, 401–424.

THOMPSON, A. B. (1976b): Mineral reactions in pelitic rocks; II. Calculation of some P-T-X (Fe-Mg) phase relations. Am. J. Sci., **276**, 425–454.

TINGEY, R. J. (1982): The geologic evolution of the Prince Charles Mountains–An Antarctic Archean cratonic block. Antarctic Geoscience, ed. by C. CRADDOCK. Madison, Univ. Wisconsin Press, 455–464.

WINDOM, K. E. and BOETTCHER, A. L. (1976): The effect of reduced activity of anorthite on the reaction grossular+quartz=anorthite+wollastonite; A model for plagioclase in the earth's lower crust and upper mantle. Am. J. Sci., **61**, 889–896.

YANAI, K., NISHIDA, T., KOJIMA, H., SHIRAISHI, K., ASAMI, M., OHTA, Y., KIZAKI, K. and MATSUMOTO, Y. (1982): The central Yamato Mountains, Massif B and Massif C, Antarctica. Antarct. Geol. Map Ser., Sheet 28 (with explanatory text 10 p., 6 pl.). Tokyo, Natl Inst. Polar Res.

YOSHIDA, M. and ANDO, H. (1971): Geological surveys in the vicinity of Lützow-Holm Bay and the Yamato Mountains, East Antarctica. Nankyoku Shiryô (Antarct. Rec.), **39**, 46–54.

YOSHIDA, M. and AIKAWA, N. (1983): Petrography of a discordant metabasite from Skallen, Lützow-Holmbukta, East Antarctica. Mem. Natl Inst. Polar Res., Spec. Issue, **28**, 144–165.

(Received May 21, 1985; Revised manuscript received June 22, 1985)